Multicomponent Molecular Conductors with Supramolecular Assembly: Iodine-Containing Neutral Molecules as Building Blocks

Hiroshi M. Yamamoto,* Jun-Ichi Yamaura, and Reizo Kato*

Contribution from The Institute for Solid State Physics, The University of Tokyo, 7-22-1 Roppongi, Minato-ku, Tokyo 106-8666, Japan

Received January 2, 1998

Abstract: Lewis acid−base interactions between anions and iodine-containing neutral molecules have been utilized in order to accomplish multicomponent molecular conductors with supramolecular assemblies. In the presence of diiodoacetylene (DIA), *p*-bis(iodoethynyl)benzene (*p*BIB), and/or tetraiodoethylene (TIE), several cation-radical salts of bis(ethylenedithio)tetrathiafulvalene (BEDT-TTF) or ethylenedithiotetrathiafulvalene (EDT-TTF) are prepared by galvanostatic oxidation with such supporting electrolytes as Cl^-, Br^-, I^-, and/or $AuBr_2^-$. Crystal structures of these salts solved by the X-ray diffraction method exhibit novel donor (BEDT-TTF or EDT-TTF) arrangements and supramolecular assemblies made of the anions and the neutral molecules (DIA, *p*BIB, and/or TIE). Transport properties show that these salts range from metal to semiconductor. Several interesting properties such as a curious band dispersion and high anisotropy in resistivity are also observed. Some packing motifs for the description of the supramolecular assemblies have been revealed by an overview of these crystal structures.

Introduction

The properties of molecule-based materials depend not only on the nature of the component molecule alone but also on the relative *arrangement* of the molecules in the crystal. Indeed, the molecular arrangement in the crystal is known to control such many properties as nonlinear optical behavior,[1] solid-state polymerization,[2] magnetism,[3] and electrical conductivity.[4] As means for developing novel molecular arrangements, supramolecular systems[5] gather attention of chemists on material science recently, because they can govern the architecture of the material. This feature of the system has contributed to contemporary progresses of the crystal engineering.[6] Therefore, the supramolecular chemistry should play an important role in the control of the molecular arrangement and thus the modification of the physical properties.

Supramolecular assembly is a rigidly organized system with *infinite* frameworks. Its control ability over the molecular arrangement is especially effective in the solid state because its rigidity and infinity restrict possible packing of the counter component. Therefore, a construction of the supramolecular assembly in the solid state is a promising pathway to new and desired materials. To construct the supramolecular assembly, several types of intermolecular interactions are utilized.[6] Among these interactions, the halogen−halogen interaction attracts less attention than such others as hydrogen bond and CH−π bond, although it has been known for a long time.[7] Recently, however, two-dimensional (2D) networks that consist of halide anions and diiodoacetylene (DIA) were reported by Ghassemzadeh *et al*.[8] In their work, Lewis-basic anions and DIA containing Lewis-acidic iodine atoms are organized by the acid−base interaction to form the 2D network. Since the interaction is strong and directional, the rigidity of the network seems to be applicable to the regulation of many kinds of molecular arrangements. Particularly, the network is suitable to control the arrangement of cation-radicals in the molecular conductors, since the network contains negatively charged ions.

Meanwhile, in the field of molecular conductors, there is another current topic apart from the supramolecular assembly. Although most donor-based molecular conductors are composed of two components (cation-radical of the donor molecule and its counteranion), cocrystallizations of the third neutral component(s) are occasionally observed. Resulting *multicomponent* systems provide some of the most interesting materials in this field. For example, recent investigations have revealed that in superconductive salts such as (BEDT-TTF)$_2$[M(CF$_3$)$_4$]-(trihaloethane) (BEDT-TTF = bis(ethylenedithio)tetrathiafulvalene; M = Cu, Ag, Au)[9] and (BEDT-TTF)$_4$[(H$_2$O)Fe(C$_2$O$_4$)$_3$]-PhCN[10] the third *neutral* component (trihaloethane, PhCN, and H$_2$O in each example) affects the crystal structure and tunes its physical properties.[9] In many multicomponent systems, how-

(1) Marder, S. R.; Sohn, J. E.; Stucky, G. D. *Materials for Nonlinear Optics*. *Chemical Perspectives*; *Adv. Chem. Ser*. 1991.

(2) Hasegawa, M. *Advances in Physical Organic Chemistry vol. 30*; Academic Press: London, 1995; pp 117−171.

(3) (a) Kinoshita, M.; Turek, P.; Tamura, M.; Nozawa, K.; Shiomi, D.; Nakazawa, Y.; Ishikawa, M.; Takahashi, M.; Awaga, K.; Inabe, T.; Maruyama, Y. *Chem. Lett.* **1991**, 1225−1228. (b) Kahn. O. *Molecular Magnetism*; VCH Verlagsgesellschaft; Weinheim, 1993.

(4) Kini, A. M.; Beno, M. A.; Carlson, K. D.; Ferraro, J. R.; Geiser, U.; Shultz, A. J.; Wang, H. H.; Williams, J. M.; Whangbo, M.-H. *The physics and chemistry of organic superconductors*: *proceedings of the ISSP International symposium*; VCH: New York, 1989; pp 334−341.

(5) For a recent review, see: Lehn, M. M. *Supramolecular Chemistry*. *Concepts and Perspectives*; VCH Verlagsgesellschaft: Weinheim, 1995.

(6) Desiraju, G. R. *The Crystal as a Supramolecular Entity* (*Perspectives in Supramolecular Chemistry vol. 2*); John Wiley & Sons: West Sussex, 1995.

(7) (a) McDaniel, D. H.; Dieters, R. M. *J. Am. Chem. Soc.* **1966**, 88, 2607−2608. (b) Creighton, J. A.; Thomas, K. M. *J. Chem. Soc., Dalton Trans.* **1972**, 403−410.

(8) Ghassemzadeh, M.; Harms, K.; Dehnicke, K. *Chem. Ber*. **1996**, *129*, 259−262.

(9) Schlueter, J. A.; Geiser, U.; Wang, H. H.; Kelly, M. E.; Dudek, J. D.; Williams, J. M.; Naumann, D.; Roy, T. *Mol. Cryst. Liq. Cryst.* **1996**, *284*, 195−202.

(10) Graham, A. W.; Kurmoo, M.; Day, P. *J. Chem. Soc., Chem. Commun*. **1995**, 2061−2062.

S0002-7863(98)00024-9 CCC: $15.00 © 1998 American Chemical Society
Published on Web 06/09/1998

ever, the neutral component comes from the solvent used for the crystal growth and is incorporated incidentally. The solvent molecules tend to be packed loosely and are often disordered. Consequently, to develop well-organized multicomponent systems, rational introduction of neutral molecules are required.

With above aspects in mind, we tried utilizing the Lewis acid−base interaction in order to introduce *neutral* molecule(s) into molecular conductors more deliberately. At the same time, by means of this interaction, we intended to fabricate supramolecular assembly in the crystal to provide new structures and properties. Although preceding research has revealed that the functionalization of donor molecules is valid for the application of the supramolecular chemistry to molecular conductors,[11] neutral molecules have never been used in this purpose. We think that the supramolecular chemistry of the *multicomponent* molecular conductors still remains unexplored and is worth challenge.

Recently, we succeeded to fabricate the supramolecular assemblies with halide anions (Cl^- or Br^-) and DIA in BEDT-TTF salts.[12] We selected DIA, tetraiodoethylene (TIE), and *p*-bis(iodoethynyl)benzene (*p*BIB) as key components for the supramolecular system in this article. Electron-deficient iodine atoms in these molecules are essential for the assembly. Lewis-acidic iodine atoms coordinate to Lewis-basic anions to form unique polymeric structures. The donor molecules BEDT-TTF and EDT-TTF (= ethylenedithiotetrathiafulvalene) are used for the formation of the conduction path. These donors are at present two of the most promising donors in the search for new metallic or superconducting salts. Moreover, they are suitable counterparts to examine ability of our supramolecular system to build new structures, because the possible molecular arrangements with discrete anions have already been investigated thoroughly. Therefore, the plentiful library of preceding investigations allows us to judge whether the formation of the obtained donor arrangement is possible without the existence of the supramolecular assembly or not. With this strategy, we have studied eight conductive cation-radical salts. In these molecular conductors, anions and iodine-containing neutral molecules form novel supramolecular assemblies: one-dimensional (1D) chains, 2D sheets, and a three-dimensional (3D) network. In addition, the assemblies yield novel donor arrangements and thus affect the physical properties of these salts.

Experimental Section

General. DIA,[13] BEDT-TTF,[14] and EDT-TTF[15] were synthesized by literature procedure. Chlorobenzene, methanol, ethanol, THF, potassium hydroxide, sodium thiosulfate, tetraphenylphosphonium chloride, *n*-butyllithium (in hexane), and tetra(*n*-butyl)ammonium bromide were purchased from Wako Chem. Co. Ltd., iodine was purchased from Kokusan Chem. Co. Ltd., and tetra(*n*-butyl)ammonium dibromoaurate were purchased from Tokyo Chem. Industry Co. Ltd., TIE was purchased from Aldrich Chem. Co., and they were used without further purification. 1,1,2-Tricholoroethane was purchased from Wako Chem. Co. Ltd. and washed successively with concentrated H_2SO_4, water, and $NaHCO_3$ aqueous, then dried with $CaCl_2$, and fractionally distilled. Standard H-shaped cells (20 mL) and platinum electrodes (1 mm in diameter) were used for galvanostatic oxidation.

***p*BIB.** To a THF (200 mL) solution of *p*-diethynylbenzene (2.65 g, 21.0 mmol)[16] was added *n*-butyllithium in hexane (1.56 N, 27.0 mL, 42.1 mmol) dropwise at −78 °C. After stirring at 0 °C for 2 h, iodine (10.72 g, 42.2 mmol) in 120 mL THF was added at −78 °C. This solution was gradually warmed to room temperature, and an aqueous solution of sodium thiosulfate (ca. 10%, 200 mL) was added portionwise. The organic layer was extracted with Et_2O (300 mL × 2), washed with brine, and dried. Purification by silica gel column chromatography with 1:1 mixture of hexane and dichloromethane as an eluent gave crude *p*BIB (3.81 g, 10.1 mmol, 48.0%). Recrystallization of the crude product from hot chloroform gave pure *p*BIB as pale yellow flakes. *m*/z: 380; 1H NMR: 7.36 (4H, s); Calc. C: 31.45, H: 1.05, N: 0.0. Found. C: 31.84, H: 1.19, N: 0.0; Mp 175 °C (dec).

Crystal Preparation: General. Galvanostatic oxidation procedures of 20 mL solutions containing the donor molecules, neutral molecules, and supporting electrolytes were performed under argon atmosphere. Constant currents were applied for several days. Crystals with enough quality for resistivity measurement and X-ray structure analysis harvested on the electrodes.

X-ray Diffraction Studies. Eight crystals obtained as described above were mounted on glass fibers using epoxy cement. X-ray diffraction data were collected on a MAC Science automatic four-circle diffractometer (MXC18), a Rigaku automatic four-circle diffractometer (AFC6S), or a MAC Science imaging plate (DIP320) with graphite-monochromated Mo K_α radiation at 293 K. The intensities were corrected for Lorentz and polarization effects. The structures were solved by a direct method and refined by full-matrix least-squares methods. For **5** and **8**, the refinements were performed using SHELXL-93.[17] Analytical absorption correction was carried out. Anisotropic thermal parameters were used for non-hydrogen atoms. All hydrogen atoms were added in calculated positions with fixed isotropic contributions. All calculations were performed with use of teXsan crystallographic software package of Molecular Structure Co. Table 1 gives crystal data for the eight compounds. *R* values for some crystals are moderately large, which would be due to poor crystal quality.

Band Calculation. To calculate intermolecular overlap integrals, HOMO obtained by the extended Hückel MO calculation was used.[18] The calculation was carried out with the use of semiempirical parameters for Slater-type atomic orbitals.[19] It has been assumed that the transfer integral (t) is proportional to the overlap integral (S), $t = \epsilon S$ ($\epsilon = -10$ eV, ϵ is a constant with the order of the orbital energies of HOMO). The band structures were calculated based on the tight-binding approximation.

Electrical Resistivity Measurements. The d.c. resistivity measurements were performed with the standard four-probe method. Gold leads (10 or 15 μm diameter) were attached to the crystal with carbon paste.

Results and Discussion

The normal galvanostatic oxidation of solutions containing donor molecules and supporting electrolytes was performed in the presence of iodine-substituted neutral molecules (DIA, *p*BIB, and/or TIE). By this procedure, $(BEDT\text{-}TTF)_2Cl(DIA)$ (**1**), $(BEDT\text{-}TTF)_2Br(DIA)$ (**2**), $(BEDT\text{-}TTF)_2Cl_2(DIA)(TIE)$ (**3**),

(11) (a) Blanchard, P.; Duguay, G.; Cousseau, J.; Sall1, M.; Jubault, M.; Gorgues, A.; Boubekeur, K.; Batail, P. *Synth. Metals.* **1993**, *56*, 2113-2117. (b) Batsanov, A. S.; Bryce, M. R.; Cooke, G.; Dhindsa, A. S.; Heaton, J. N.; Howard, J. A. K.; Moore, A. J.; Petty, M. C. *Chem. Mater*. **1994**, *6*, 1419−1425. (c) Dolbecq, A.; Fourmigue, M.; Batail, P.; Coulon, C. *Chem. Mater*. **1994**, *6*, 1413−1418. (d) Neilands, O.; Belyakov, S.; Tilika, V.; Edzina, A. *J. Chem. Soc., Chem. Commun*. **1995**, 325−326. (e) Imakubo, T.; Sawa, H.; Kato, R. *J. Chem. Soc., Chem. Commun.* **1995**, 1097−1098. (f) Imakubo, T.; Sawa, H.; Kato, R. *Synth. Metals* **1995**, *73*, 117−122. (g) Imakubo, T.; Sawa, H.; Kato, R. *J. Chem. Soc., Chem. Commun*. **1995**, 1667−1668.

(12) Yamamoto, H. M.; Yamaura. J.; Kato. R. *J. Mater. Chem*. **1998**, 15−16.

(13) Franzen, V. *Chem. Ber*. **1954**, *87*, 1148−1154.

(14) (a) Svensrup, N.; Becher, J. *Synthesis* **1995**, 215−235. (b) Engler, E. M.; Lee, V. Y.; Schumaker, R. R.; Parkin, S. S. P.; Greene, R. L.; Scott, J. C. *Mol. Cryst. Liq. Cryst.* **1984**, *107*, 19−31.

(15) Kato, R.; Kobayashi, H.; Kobayashi, A. *Chem. Lett.* **1989**, 781−784.

(16) Takahashi, S.; Kuroyama, Y.; Sonogashira, K.; Hagihara, N. *Synthesis* **1980**, 627−630.

(17) Sheldrick, G. M. Program for the Refinement of Crystal Structures; University of Goettingen: Germany, 1993.

(18) Mori, T.; Kobayashi, A.; Sasaki, Y.; Kobayashi, H.; Saito, G. *Bull. Chem. Soc. Jpn*. **1984**, *57*, 627−633.

(19) Canadell, E.; Rachidi, I. E.-I.; Ravy, S.; Pouget, J. P.; Brossard, L.; Legros, J. P. *J. Phys. France* **1989**, *50*, 2967−2981.

Table 1. Crystallographic Parameters

crystal	**1**	**2**	**3**	**4**	**5**	**6**	**7**	**8**
empirical formula	$C_{22}S_{16}H_{16}I_2Cl$	$C_{22}S_{16}H_{16}I_2Br$	$C_{24}S_{16}H_{16}I_6Cl_2$	$C_{24}S_{16}H_{16}I_6Br_2$	$C_{66}S_{48}H_{48}Au_6Br_{13}I_{12}$	$C_{40}S_{24}H_{28}ClI_2$	$C_{34}S_{24}H_{24}B_{r2}I_7$	$C_{42}H_{24}S_{24}BrI_{22}$
formula weight	1082.59	1127.04	1649.68	1738.59	6123.39	1567.36	2250.14	4169.89
crystal system	triclinic	triclinic	triclinic	triclinic	monoclinic	triclinic	monoclinic	tetragonal
a/Å	7.642(3)	7.743(1)	10.179(2)	10.283(2)	34.278(4)	10.184(3)	32.090(4)	23.435(10)
b/Å	17.477(6)	17.651(2)	13.857(2)	13.905(3)	25.412(3)	15.578(4)	13.932(2)	
c/Å	6.728(3)	6.739(9)	7.929(2)	7.966(2)	7.954(2)	9.258(3)	15.307(2)	8.130(3)
α/deg	99.49(3)	99.82(1)	95.81(2)	96.04(2)		99.73(2)		
β/deg	104.90(3)	106.90(1)	100.59(2)	100.49(2)	93.268(13)	106.87(2)	117.54(1)	
γ/deg	83.20(3)	82.39(1)	80.10(1)	80.48(2)		76.33(3)		
V/Å^3	853.8(6)	864.9(2)	1080.3(4)	1101.2(4)	6917.50(18)	1357.7(8)	6068(1)	4464(1)
space group	$P\bar{1}$	$P\bar{1}$	$P\bar{1}$	$P\bar{1}$	$C2/m$	$P\bar{1}$	$C2/c$	$P42_12$
Z	1	1	1	1	2	1	4	2
D_{calc} (D_{obs})/g cm^{-3}	2.105	2.164	2.536	2.621	2.940 (2.95(1))	1.917	2.463	3.101 (3.11(1))
$2\theta_{max}$/deg	55	55	65	70	55	61.0	60.5	60.1
color	dark brown	black	black	black	black	black	black	black
goodness of fit	7.18	5.46	4.77	5.92	0.95	5.77	2.53	1.10
R^a,R_w^b	0.095; 0.093	0.079; 0.078	0.046; 0.057	0.055; 0.057	0.096; 0.266	0.097; 0.106	0.037; 0.039	0.074; 0.247

[a] $R = \sum||F_o| - |F_c||/\sum|F_o|$. [b] $R_w = [\sum w(F_o^2 - F_c^2)^2/\sum w(F_o^2)^2]^{1/2}$, $w = [\sigma_c^2(F_o) + (aP)^2]^{-1}$ where $P = (F_o^2 + 2F_c^2)/3$, for **5** and **8**; $R_w = [\sum w(|F_o| - |F_c|)^2/\sum w|F_o|^2]^{1/2}$, $w = [\sigma_c^2(F_o) + p^2F_o^2/4]^{-1}$, for others.

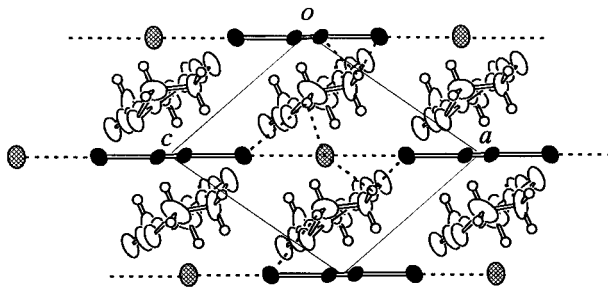

Figure 1. Crystal structure of (BEDT-TTF)$_2$Cl(DIA) (**1**) viewed along the longitudinal axis of BEDT-TTF. Shorter contacts than van der Waals contacts are presented as dotted lines.

(BEDT-TTF)$_2$Br$_2$(DIA)(TIE) (**4**), (BEDT-TTF)$_6$(AuBr$_2$)$_6$Br(TIE)$_3$ (**5**), (BEDT-TTF)$_3$Cl(*p*BIB) (**6**), (EDT-TTF)$_4$Br$_2$I$_3$(TIE) (**7**), and (EDT-TTF)$_4$BrI$_2$(TIE)$_5$ (**8**) were obtained. X-ray structure analyses were performed on these cation-radical salts. In every crystal, the neutral molecules coordinate to the anions and form novel supramolecular structures. The distances between the anions and the neutral iodine atoms are quite shorter than the corresponding van der Waals contacts. These characteristically short and directional contacts should originate from the strong Lewis acid−base interaction between anions and electron-deficient iodine atoms. In addition, there was no iodine atom without coordination. The iodine atoms coordinate to only one anion in all the cases. It is notable that no polymorph was observed in every batch. Furthermore, Cl^- and Br^- analogues form isomorphous structures in all the cases (**1** and **2**; **3** and **4**).[20] Because the oxidation potential of I^- is lower than that of BEDT-TTF, no I^- analogue has been obtained for BEDT-TTF salts.

Crystal Structures

(BEDT-TTF)$_2$X(DIA) (X = Cl, Br; 1 and 2). The crystal structure of **1** is shown in Figure 1. The crystal **2** is isomorphous with **1**. The most striking feature is that these crystals show finely organized structure fabricated by the anions and the neutral molecules: the DIA and the halide anions stand in a line alternately to compose a 1D chain. The interatomic Cl···I distance (3.041(1) (Å) in **1** is remarkably shorter than the sum (3.65 Å) of the anion radius of Cl^- (1.67 Å)[21] and the van der Waals radius of I (1.98 Å).[22] The Br···I distance in **2** is 3.156(1) Å that is also much shorter than the sum of the anion radius and the van der Waals radius ($r(Br^-) + r(I) = 3.80$ Å). It should be mentioned that the halide anions and DIA molecules form the 2D sheets in the crystals reported by Ghassemzadeh et al.[9] This difference in configuration indicates that DIA forms various kinds of network structures depending on counterparts and circumstances in the crystals.

Two donor molecules in the unit cell are interrelated by an inversion center, and both Cl^- and DIA are on inversion centers. The projection of the donor molecules along their longitudinal axes resembles that of the previously reported *β*"-(BEDT-TTF)$_2$AuBr$_2$. This donor arrangement is a new variety of *β*"-type.[23] It is noteworthy that the donor molecules fit into the channels formed by the 1D chains along the "***a*** − ***c***" direction. The C−C bonds of the terminal ethylene groups of BEDT-TTF are almost parallel to the 1D chains. Several distances between the terminal hydrogen atoms and 1D chains are short enough to be regarded as van der Waals contacts. These short contacts seem to align BEDT-TTF molecules parallel to the 1D chains. In contrast to the strong interaction within the chain, there is no van der Waals contact between the chains. This absence of short interchain contact indicates that the distance between the chains is dominated by the period of the donor arrangement.

(BEDT-TTF)$_2$X$_2$(DIA)(TIE) (X = Cl, Br; 3 and 4). The crystal structure of **4** is shown in Figure 2. The crystal **3** is isomorphous with **4**. There are corrugated 2D sheets constructed by the Br^- anions, DIA, and TIE molecules. These 2D sheets penetrate into the conduction layers, which is an unusual feature in BEDT-TTF salts. The donor molecules are dimerized, and two molecules in the dimer are interrelated by an inversion center. Both DIA and TIE are on the inversion centers. Two TIEs and four DIAs surround the dimer of donor molecule. Many short C−H···X contacts as well as a short S···Br contact are observed.

It is noteworthy that one of the terminal dithiin groups in the BEDT-TTF molecule exhibits a boat-type conformation. It

(20) We also obtained Br^- analogue of the crystal **6**. The cell parameters are as follows: triclinic, $a = 10.189(2)$, $b = 15.423(2)$, $c = 9.417(2)$ Å, α = 99.81(1), $\beta = 106.91(1)$, $\gamma = 77.18(1)°$, $V = 1371.6(4)$ Å^3.

(21) Shannon, R. D. *Acta Crystallogr. Sect. A* **1976**, *32*, 751−767.
(22) Bondi, A. *J. Phys. Chem.* **1964**, *68*, 441−451.
(23) Mori, T.; Sakai, F.; Saito, G.; Inokuchi, H. *Chem. Lett.* **1986**, 1037−1040. Both arrangements in the salts **1** and **6** are two of new varieties of the *β*"-type arrangement. The main difference between the original *β*"-type arrangement and those reported in this article lies in the displacement pattern along their longitudinal axes. (Personal communication with Prof. Takehiko Mori.)

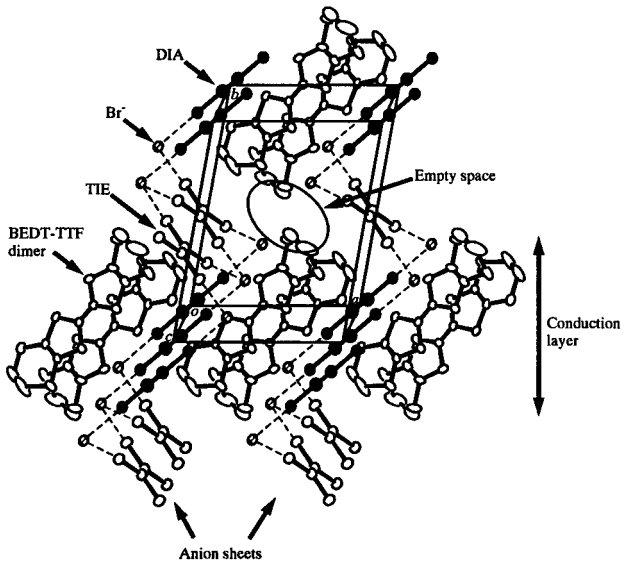

Figure 2. Crystal packing of $(BEDT\text{-}TTF)_2Br_2(DIA)(TIE)$ (**4**). Hydrogen atoms are omitted for clarity.

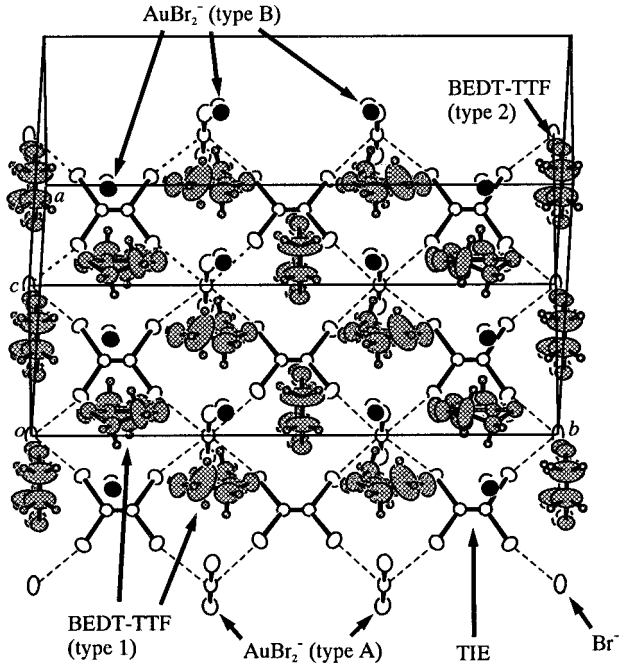

Figure 3. Crystal packing of $(BEDT\text{-}TTF)_6(AuBr_2)_6Br(TIE)_3$ (**5**) viewed along the longitudinal axes of the donor molecules.

seems that this anomalous conformation arises from two reasons. The empty space at the center of the unit cell, indicated in Figure 2 as an ellipse, is filled by the ethylene group to optimize crystal packing. At the same time, this anomalous conformation leads to the contraction of the BEDT-TTF molecule and adjusts a discrepancy in length between the DIA unit and the donor molecule. Therefore, this anomaly suggests that the rigidly organized anion network affects the donor conformation.

$(BEDT\text{-}TTF)_6(AuBr_2)_6Br(TIE)_3$ (5). The crystal structure of **5** is shown in Figure 3. $AuBr_2^-$, Br^-, and TIE molecules construct 2D sheets. There are two types of $AuBr_2^-$ anions: the one (type A) is coordinated by four TIEs at the central Au atom and incorporated in the sheet; the other (type B) is located apart from the sheets and incorporated in the conduction layer. Both kinds of $AuBr_2^-$ anions are almost perpendicular to the 2D sheets. There is no short contact between these two types of $AuBr_2^-$ anions, which indicates that an interaction between

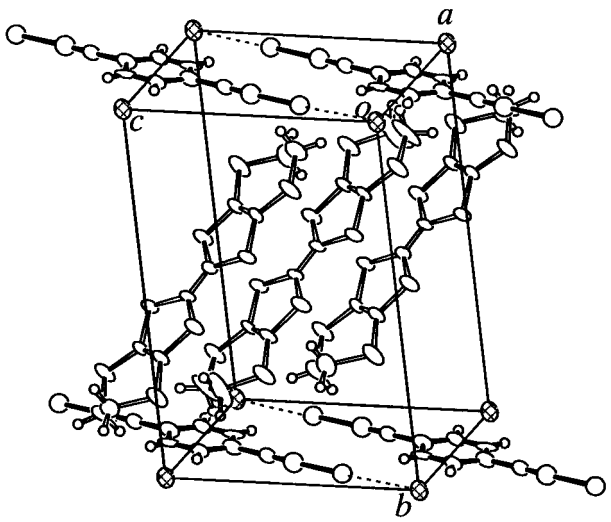

Figure 4. Crystal packing of $(BEDT\text{-}TTF)_3Cl(p\text{BIB})$ (**6**).

Lewis-bases should be weak. The Br^- anion exhibits an elongated thermal ellipsoid presumably because of the thermal vibration. In the course of the crystal structure analysis, the occupancy for Br^- was refined, and we obtained the value close to 1.0. Therefore, the occupancy for Br^- was fixed to 1.0, which is consistent with the observed density of the crystal (Table 1). Donor molecules are arranged so that they surround the $AuBr_2^-$ anion (type B). One complete (type 1) and half (type 2) donor molecules are crystallographically independent. The type 2 molecule is on a mirror plane. According to the equation proposed by P. Guionneau et al.,[24] the formal charges of these two types of donor molecules are calculated to be 1.8 (type 1) and 1.3 (type 2), respectively. Because of the distorted molecular shape of the type 1 molecule, the value for the type 1 molecule is not very reliable. Judging from the value of 1.3 for the type 2 molecule and the average formal charge of +7/6, however, there seems little charge separation between these two types of molecules.

The two types of donor molecules are perpendicular to one another. There is neither column structure nor dimerization of the donor. This is similar to the τ-type structure as seen in τ-(P−(S,S)-DMEDT-TTF)$_2$(AuBr$_2$)$_1$(AuBr$_2$)$_{\sim 0.75}$.[25] In the case of the P−(S,S)-DMEDT-TTF salt, however, the τ-type architecture is mainly due to the nature of the donor molecules: two methyl groups on the terminal ethylene and the attractive S···N interactions.

$(BEDT\text{-}TTF)_3Cl(p\text{BIB})$ (6). The crystal structure is shown in Figure 4. The Cl^- and *p*BIB form 1D chains, similar to those in the crystal **1**. Through very short interhalogen contacts (3.13 Å), they stand in a line alternately. Both Cl^- and *p*BIB are on inversion centers. One and half donor molecules are crystallographically independent, with one molecule on general position and a half molecule on an inversion center. The projection of the donor molecules along their longitudinal axes resembles that of the previously reported β"-$(BEDT\text{-}TTF)_2AuBr_2$. This donor arrangement is another new variety of the β"-type, similar to those in the salt **1**.[23] A difference between the arrangements of salt **1** and **6**, however, exists: In the unit cell, there are three donor molecules, whereas the unit cell of **1** accommodates two

(24) Guionneau, P.; Kepert, C. J.; Chasseau, D.; Truter, M. R.; Day, P. *Synth. Metals* **1997**, 479−480.

(25) (a) Papavassiliou, G. C.; Terzis, A.; Zambounis, J. S.; Delhaes, P.; Murata, K.; Fortune, N. A.; Shirakawa, N. *Synthetic Metals* **1995**, *70*, 787−788. (b) Zambounis, J. S.; Papavassiliou, G. C.; Murata, K. *Solid State Commun.* **1995**, *95*, 211−215.

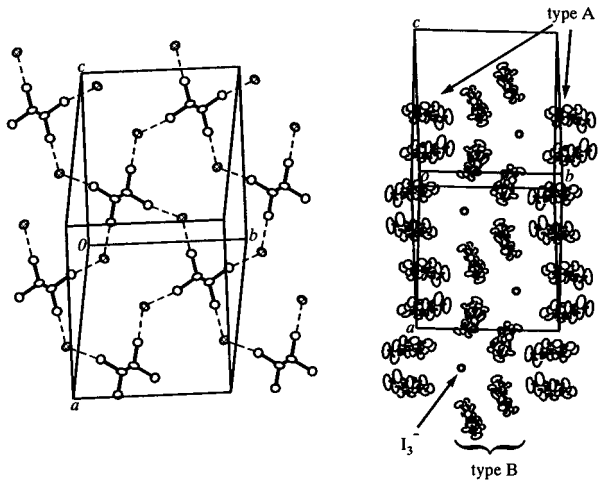

Figure 5. Anion sheet (left) and donor arrangement (right) in the crystal $(EDT\text{-}TTF)_4Br_2I_3(TIE)$ (**7**). Hydrogen atoms are omitted for clarity.

donor molecules. This increase of the number can be attributed to the difference in the length between DIA and *p*BIB. In fact, the distance between two Cl^- anions within the chain is 1.5 times longer than that of **1** (11.4 and 18.4 Å for **1** and **6**, respectively). Another difference between **1** and **6** is the angle between the molecular plane and the pseudo-stacking direction: 58° for **1** and 77° for **6**.

Although the donor molecules are also aligned along the 1D chain, there are very few contacts between the terminal ethylene group and the anion framework. On the other hand, interchain H···I and H···Cl contacts (3.34 and 2.89 Å, respectively) are observed, which suggests that these transverse contacts determine the interchain distance of 4.8 Å. This architecture makes contrast to that of the 1D chain with DIA and Cl^- of which interchain distance is dominated by the interaction with the donor molecules.

The calculations of the charges of these donors from their bond lengths result in 0.4 and 0.3 for the one and half donor molecules, respectively. This suggests an existence of little charge separation. The angle between the longitudinal axes of the donor molecules and the normal line of the anion layer is about 40°. This angle is very large as compared to those in other BEDT-TTF salts.

$(EDT\text{-}TTF)_4Br_2I_3(TIE)$ (7). The crystal structure is shown in Figure 5. There are planar 2D sheets constructed by the Br^- and TIE. Two TIEs coordinate to one Br^-. There are two sheets in the unit cell that are interrelated by inversion centers. Between these sheets, linear I_3^- anions stand like pillars, and three dimers of the donor molecules (= EDT-TTF) surround each of them. There are two crystallographically independent donor molecules, and both form dimers by the inversion operation. Type A dimers stack to form 1D columns, and type B dimers are located between the columns. The dimers of each type are interrelated by the 2-fold rotation axis. As a result, very unique donor arrangement is achieved. Judging from the bond lengths, these two types of donor molecules are different in their formal charge. Their formal charges are roughly estimated according to the equation proposed by P. Guionneau *et al.*[24] for BEDT-TTF. The charge for type A is 0.45, and that for type B is 0.86. The averaged charge is 0.66, which is comparable to the formal charge (= 0.75) calculated by the crystal formula.

$(EDT\text{-}TTF)_4BrI_2(TIE)_5$ (8). The supramolecular structure is shown in Figure 6. There is a 3D network constructed by Br^-, I^-, and TIE. 1D columns of the donor molecules run

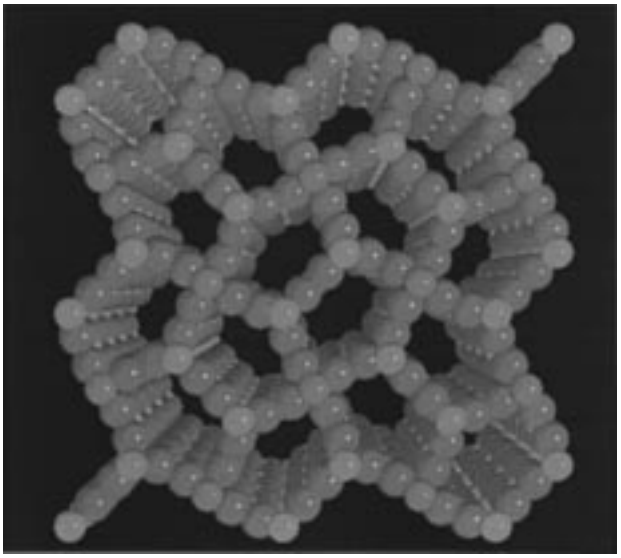

Figure 6. Space-filling model of 3D network with Br^- (red), I^- (blue), and TIE (green for iodine and gay for carbon atoms) in $(EDT\text{-}TTF)_4BrI_2(TIE)_5$ (**8**).

through channels in the 3D network. Each donor molecule is interrelated by 2-fold axes and 4-fold axes. There exist two independent TIE molecules: the one on a 2-fold axis coordinates to four I^-, while the other at general position coordinates to two Br^- and two I^-. As for the donor molecules, there is an orientational disorder with two possible tilting modes against the ***c*** axis. The angles between the ***c*** axis and the normal lines of the donor planes are ±30°. In the process of the structure analysis, the EDT-TTF unit was refined as two superimposed molecules. The bond lengths of these two donors are constrained to be the same. The populations for these two molecules are refined, and the resulting occupancies are about 0.5 for both. Since the coexistence of these two orientations in one channel is unlikely, one column is expected to be composed of the donors with only one orientation. We are convinced of this disorder by observing diffuse streaks in the ***a**** and ***b**** directions. This disorder suggests that each donor column is isolated from others by the supramolecular framework.

Overview of Molecular Packing

It would be very difficult to achieve novel donor arrangements described above without the supramolecular anion frameworks. Packing analysis of these salts should lead to the factors that govern the structural details of the multicomponent molecular conductors. We now describe some general packing motifs, with which the compatibility between donors and anion framework is accomplished so that both parts form the same crystallographic periodicity.

Before discussion on the compatibility, it would be better to mention the size of "unit". By the word "unit", we mean the complex of the neutral molecules *and* the associated anions. In most cases, the size of a DIA unit or a TIE unit shows little change. The dimension definitions are shown in Figure 7. The length of the DIA unit gets longer with an increase of the anion size. We can also see a similar trend for the TIE unit. In addition, the width is more flexible than the length (The width varies from 8.0 to 9.5 Å while the length varies from 7.8 to 8.5 Å only.). The sizes of the units, however, do not drastically change. This is the same with the donor molecules. The sizes of the donor molecules neither change drastically (Figure 7).

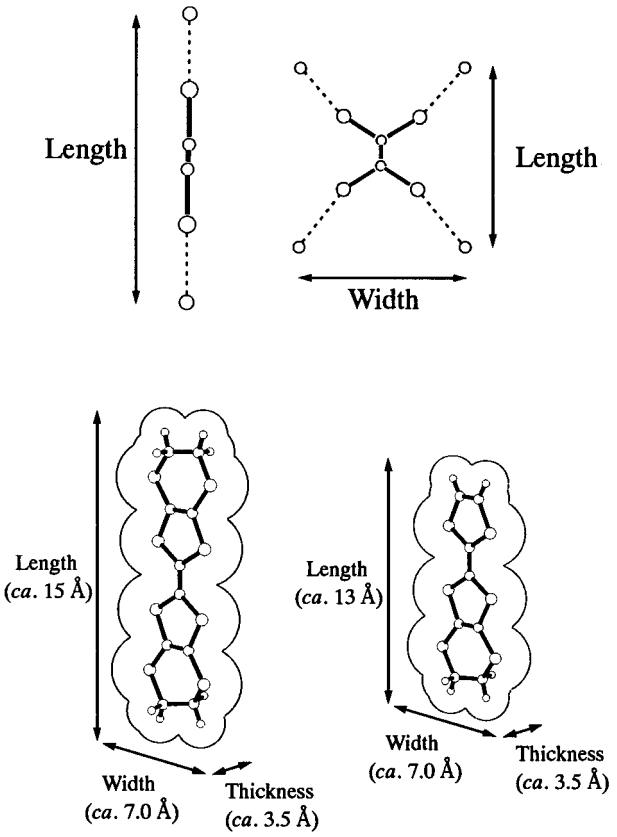

Figure 7. Dimension definition for the DIA unit, the TIE unit, and the donors. The width, thickness, and height of the donors are obtained by adding van der Waals radii to the distances between the atomic positions.

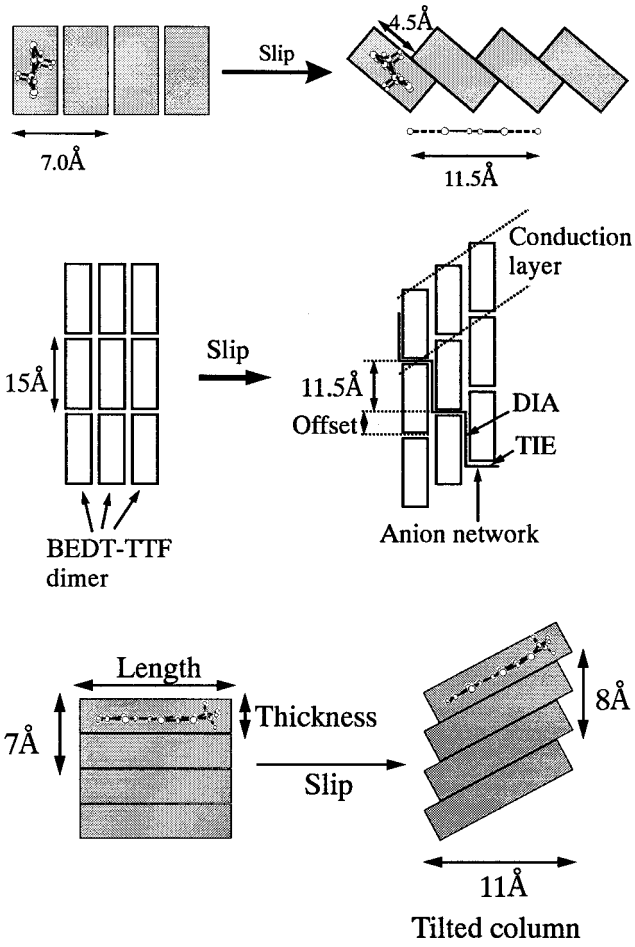

Figure 8. Schematic representation of donor arrangements and the anion networks in the crystals **1** (upper), **4** (middle), and **8** (lower).

As mentioned above, the sizes and shapes of the "units" as well as donor molecules exhibit small change. Since the anion units are connected with one another to form a polymeric configuration, this stiffness of the unit size results in the rigidity of the total anion framework in contrast to discrete anions (for example, PF_6^-, ClO_4^-, ..., etc.). Therefore, to achieve compatibility between the anion part and the donor part, arrangements of donor molecules and an interrelation between the donor and anion layers should be important.

Three types of packing motifs occur to accomplish the compatibility. The first one is "penetration" of the linear anion into the donor layer, the second one is "slip" of the donor array, and the third one is "rotation" of the donor around its longitudinal axis.

The penetration is seen in the crystals **3**−**5** and **7**. In these crystals, the linear anions are inserted among the donor molecules and tune the interval among the donors to the size of TIE. By the penetration, cylindrical spaces of 3.5 Å in diameter are filled up.

The slip of donor molecules occurs in the crystals **1**−**6**, and **8**. Two types of slips, the transverse (**1**, **2**, and **6**) and longitudinal (**3**, **4**, **6**, and **8**) ones, are observed. In the crystals **1** and **2**, the size of the BEDT-TTF unit (i.e., the width (ca. 7 Å), the thickness (ca. 3.5 Å), and the length (ca. 15.5 Å)) does not fit with the length of the DIA unit (ca. 11.5 Å). But, by the transverse slip of 4.5 Å, the period of the donor units are adapted to the length of the DIA unit (11.5 Å). Figure 8 (upper) shows the schematic representation of this process. In contrast to similar slips in other BEDT-TTF salts with discrete anions, it is interesting that the degree of the slip is determined by the period of the 1D chain. In the crystals **3** and **4**, the longitudinal slip helps the aforesaid penetration. The donor dimers slip to leave longitudinal offsets, which effectively adjusts the period of the donor arrangement to that of anion network (Figure 8: middle). In the column of EDT-TTF in **8**, the EDT-TTF molecules also slip along its longitudinal axis so that the donor period along the ***c*** axis (= stacking axis) fits into the length of the TIE unit (Figure 8: lower). At the same time, the size of the donor column fits into the longer diameter (ca. 11 Å) of the channel in the supramolecular network. The donor molecules in the crystal **6** exhibit both transverse and longitudinal slips. As seen in the crystals **1** and **2**, the degree of the transverse slip is determined by the period of the 1D chain formed by Cl^- and *p*BIB. The rather large longitudinal slip adjusts the period of the donor arrangement in the pseudostack direction to the interchain distance (4.8 Å) as mentioned before.

The rotation can be found in the crystals **5** and **7**. In the crystal **5**, the rotation of the donor as well as the penetration tunes the interval among the BEDT-TTF units to the size of the TIE unit. By means of the 90°−rotation of the BEDT-TTF molecule, the interval between the donor units can be tuned with both of their width and thickness. Furthermore, the 90°−rotation provides a cross-junction where four BEDT-TTF molecules meet. This junction affords flexible adjustment of the interval (ca. 1.0−2.0 Å). In the crystal **7**, the 60°−rotation of the donor dimer provides similar adjustment.

Electrical Resistivity

The temperature dependence of the d.c. resistivities (ρ) of the single crystals was measured by the standard four-probe

method. The crystals **1**, **2**, and **6** remain metallic down to 1.6 K. It should be noted that the ρ(r.t.)/ρ(4.2 K) ratio is fairly large for **2** (ca. 1500). The crystals **3**, **4**, **7**, and **8** are semiconductors with activation energies of 0.08, 0.15, 0.22, and 0.027 eV, respectively. The salt **5** shows high conductivity with small temperature dependence down to 50 K, which indicates a weakly metallic character. Below this temperature, the resistivity shows gradual increase with an activation energy of 0.009 eV. To our knowledge, this is the first (weakly) metallic BEDT-TTF salt with a formal charge exceeding +1.

A very high anisotropy is observed in the resistivity of **8**. At room temperature, the resistivity along the ***c*** axis (stacking axis) is 0.1 Ωcm, whereas that perpendicular to the ***c*** axis is 200 Ωcm. This anisotropy is 10 times as high as that of TTF-TCNQ[26] that is a typical 1D organic conductor. Apparently, this high anisotropy is due to the supramolecular system in the salt. It seems that conduction electrons are confined in the 1D column by the surrounding $BrI_2(TIE)_5$ wall. In other words, the salt **8** is a very pure 1D system that can be a good candidate for a theoretical model. The 1D conductor including carbon nanotube[27] gathers current interests because its nature is very different from 2D or 3D conductors, and it has potentiality to exhibit many physical phenomena such as spin-Peierls transition, Peierls transition, Tomonaga-Luttinger liquid,[28] and so on.[29]

Band Calculation

In the previous section, we have observed that many novel donor arrangements are induced by supramolecular network. To examine the effect of these novel donor arrangements on the electronic structures, band calculations based on tight-binding approximation were carried out for the metallic salts **1**, **2**, **5**, and **6**. For the calculation, overlap integrals among HOMOs of the donor molecules were estimated using the extended Hückel MO analysis. The results are shown in Figure 9.

As for **1** and **2**, the situation is very similar to each other. Two strong interactions (***r*** and ***s***) are observed along the direction parallel to the 1D chain. The Fermi surface is a distorted cylinder (Figure 9a).[30] The band structure is considerably different from that of the β"-type which exhibits a coexistence of 1D and small 2D Fermi surfaces.[23]

The overlap integrals and band structure for **5** are shown in Figure 9b. In the calculation, the HOMO levels of the two types of donor molecules are assumed to be the same because of little charge separation aforementioned. The exotic 2D donor arrangement provides very unique Fermi surface. As for the band dispersion, there are bonding, antibonding, and nonbonding bands. Since the formal charge of BEDT-TTF is +7/6, the nonbonding band is quarter-filled. Very interesting is that the width of this band is rather narrow. This situation attracts a great degree of attention because it will provide an stage for superconductivity: the narrow band leads to high density of states which is advantageous for superconductivity.[31] And this narrowness is also beneficial for a stage of itinerant ferromagnetism.[32] These expectations, however, compete with the charge localization due to the strong correlation effect. Conductivity measurement under high pressure and magnetic susceptibility measurement of this salt are now in progress.

The overlap integrals and band structure for **6** are shown in Figure 9c. In the calculation, the HOMO levels of the two types of donor molecules are also assumed to be the same. Since the crystal architecture resembles that of the crystal **1**, comparison of the band structures of the salts **1** and **6** should be discussed. The interactions ***r1*** and ***r2*** correspond to ***r*** and ***s*** in the salt **1**. These interactions along the 1D chain are strong in both salts. But the interactions ***p*** and ***q*** are quite different from each other. The value of ***p*** and ***q*** in **6** are comparable to ***r1*** and ***r2***, whereas those in **1** are about 3 times smaller than ***r*** and ***s***. As a consequence, the salt **6** shows stronger 2D character than **1** as shown in the shape of the calculated Fermi surface. The ratios between the long and short axes of the ellipses in Figure 9 (parts a and c) are 2.1 and 1.5, respectively. The enhancement of the interactions ***p*** and ***q*** seems to originate from the difference of the interplane distance of the donor molecules (about 3.90 and 3.75 Å for **1** and **6**, respectively).

Characters of Coordination

The characters of coordination as well as the dimensionality of the network are summarized in Table 2, which shows us several tendencies. At first, an increase of the distance between the anion and the iodine atom occurs when the coordination number of the anion increases (compare the distances in the table: Cl/DIA (**1**, **3**, and $PPh_4[Cl(DIA)_2]$), Br/DIA (**2**, **4**, and $PPh_4[Br(DIA)_2]$), and Br/TIE (**5**, **6**, and **8**).). This observation is rationalized as an inductive effect. Since the coordination of many iodine atoms reduces the negative charge of the anion, the Lewis acid−base interaction becomes weak to result in the increase of the distance. Second, as the atomic number of the halide anion increases, the distance also increases. For example, substitution of the Br^- for the Cl^- in **1** increases the distance between X^- and DIA from 3.04 to 3.16 Å (see **1** and **2**). Similar trend is also seen for X/TIE series (X = Cl, Br, I). This is, in a sense, a matter of course because the ion radius increases according to the atomic number. The behavior of the reduction ratio, however, is not trivial. The reduction ratio is defined as $(s-d)/s$, where s is the sum of the van der Waals radii and d is the distance between the anion and the iodine atom. The reduction is enhanced with the increase of the atomic number (compare **1** and **2**; **3** and **4**; $PPh_4[X(DIA)_2]$ where X = Cl, Br, I). The reason for this phenomenon is not certain, but the softness of the anion may be responsible for it. Because the present iodine atom is a soft Lewis-acid, it prefers interaction with "softer" Lewis-bases or anions with greater atomic number. As a consequence, the reduction is enhanced with heavier

(26) Ishiguro, T.; Kagoshima, S.; Anzai, H. *J. Phys. Soc. Jpn.* **1976**, *41*, 351−352.

(27) (a) Iijima, S. *Nature* **1991**, *354*, 56−58. (b) Ebbesen, T. W.; Lezec, H. J.; Hiura, H.; Bennett, J. W.; Ghaemi, H. F.; Thio, T. *Nature* **1996**, *382*, 54−56. (c) Tans, S. J.; Devoret, M. H.; Dai, H.; Thess, A.; Smalley, R. E.; Geerligs, L. J.; Dekker: C. *Nature* **1997**, *386*, 474−477.

(28) For reviews, see: (a) Sflyom, *J. Adv. Phys.* **1979**, *28*, 201−303. (b) Haldane, F. D. M. *J. Phys. C* **1981**, *14*, 2585−2609.

(29) For recent review of the 1D conductor, see: Roth, S. *One-Dimensional Metals Physics and Material Science*; VCH: Weinheim, 1995.

(30) In the previous communication, we reported the 1D Fermi surface for **1** and **2**.[12] Very recently, however, S. Uji et al have observed ADMRO (= Angle Dependent MagnetoResistance Oscillation) for **2** which suggests an existence of 2D Fermi surface (private communication). We have reexamined semiempirical parameters for Slater-type atomic orbitals for the sulfur atom and found that those in ref 19 give a satisfactory result that well explains the shape of the Fermi surface estimated by ADMRO. In this process, we have noticed that the dimensionality of the electronic structure associated with this type of donor arrangement is very sensitive to the intermolecular interactions, especially the ones designated "***c***", "***p***", and "***q***" in Figure 9a.

(31) According to the BCS theory, the critical temperature of the superconductivity is proportional to $\exp(-1/N)$, where N is the density of state at the Fermi level. Therefore, the higher density of states results in the higher critical temperature. (See: Bardeen, J.; Cooper, L. N.; Schrieffer, J. R. *Phys. Rev.* **1957**, *108*, 1175−1204.)

(32) (a) Lieb, E. H. *Phys. Rev. Lett.* **1989**, *62*, 1201−1204. (b) Mielke, A. *J. Phys. A* **1991**, *24*, L73, 3311−3321. (c) Mielke, A. *Phys. Lett. A* **1993**, *174*, 443−448. (d) Tasaki, H. *Phys. Rev. Lett.* **1992**, *69*, 1608−1611.

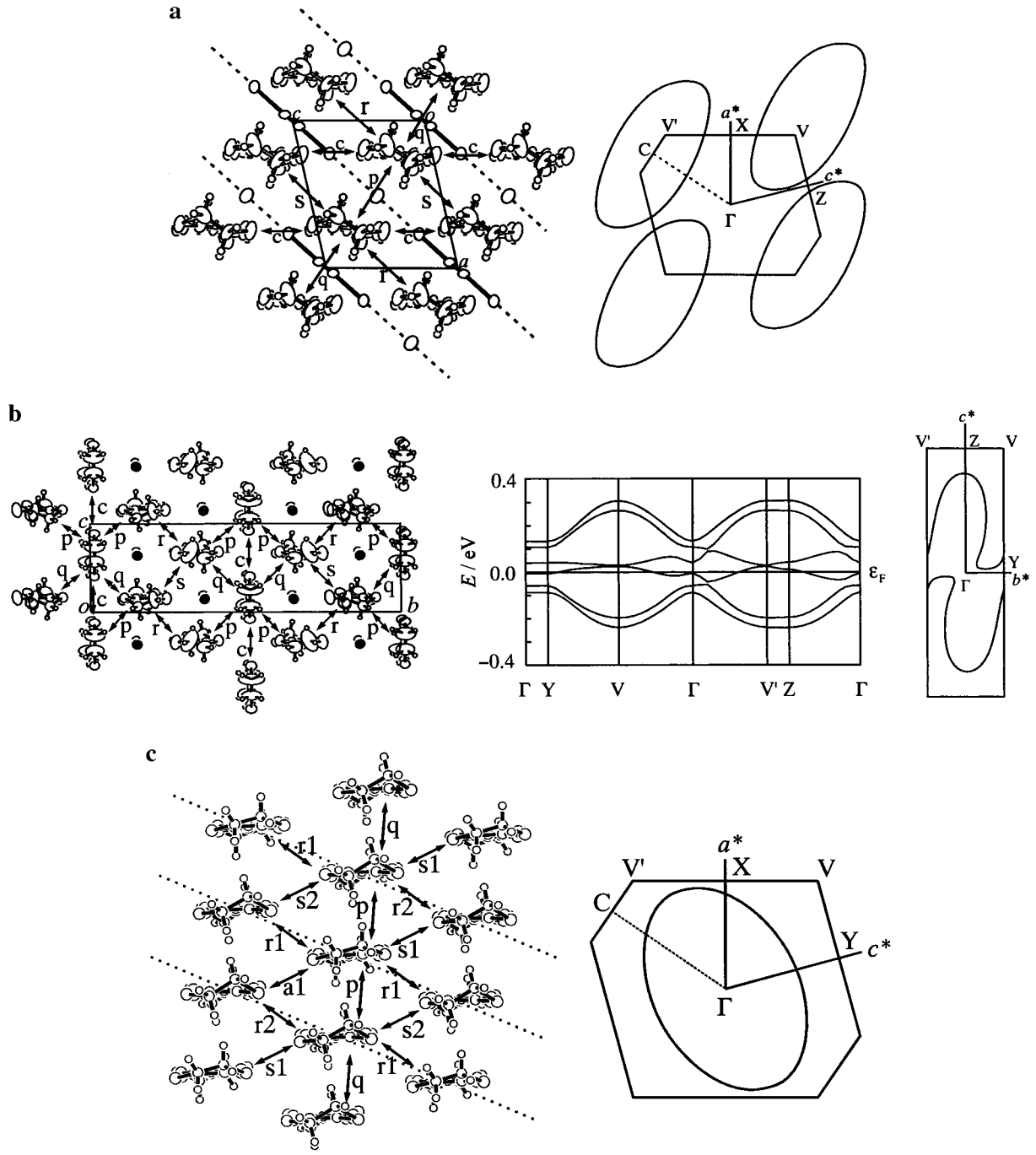

Figure 9. (a) Donor arrangement (left) and calculated Fermi surface (right) for the salt **1**. Alphabetic letters in the left figure indicate the overlap integrals ($S/10^{-3}$) of which values are as follows: S(c) = 1.63, S(p) = 1.72, S(q) = 2.42, S(r) = −4.99, S(s) = −4.80, for **1**; S(c) = 1.45, S(p) = 1.34, S(q) = 1.67, S(r) = −4.91, S(s) = −4.99, for **2**. The Fermi surface for the salt **2** is very similar to this one. (b) Donor arrangement (left), band structure (middle), and calculated Fermi surface (right) for the salt **5**. Alphabetic letters in the left figure indicate overlap integrals ($S/10^{-3}$) of which values are as follows: S(c) = 0.36, S(p) = 5.39, S(q) = −5.46, S(r) = −2.22, S(s) = −2.92. (c) Donor arrangement (left) and calculated Fermi surface (right) for the salt **6**. The dotted lines in the left figure represent the 1D chains of Cl^- and *p*BIB. Alphabetic letters indicate overlap integrals ($S/10^{-3}$) of which values are as follows: S(r1) = −5.09, S(r2) = −5.08, S(s1) = −1.12, S(s2) = −1.47, S(p) = −5.08, S(q) = −5.79.

anions. Third, the distance between the anion and DIA is shorter than that of TIE. The electron-deficiency is responsible for this trend. The iodine atoms in DIA are more electron-deficient than those in TIE because the *sp* carbon has stronger electron-withdrawing nature than the sp^2 carbon. Therefore, the stronger interactions with DIA lead to shorter distances. Finally, the coordination number increases with the dimensionality. When the supramolecular system is 1D, the coordination number is two (**1**, **2**, and **6**). On the 2D networks, the coordination number varies from two to four (**3**−**5**, **7**, $PPh_4[X(DIA)_2]$). The number of coordination in the 3D network ranges between six and eight (**7**). The coordination angles around the anions do not, however, have apparent relation with the coordination number. For example, the angle with which the two iodine atoms coordinate to the Br^- in the crystal **7** is 126°, while the angle in the crystal **1** is 180°. Similar phenomenon is also observed between the angles in the crystal **5** and $PPh_4[Br(DIA)_2]$, with the coordination number four. These observations indicate unique character of the coordination, which does not agree with the normal coordination rules such as the electron-repulsion theory.

We now focus on the structures of the supramolecular assemblies in terms of the coordination motif. Since the size

Table 2. Character of the Coordination

crystal	X	neutral molecule	coordination no.[a]	coordination angle,[b] deg	distance/Å	reduction ratio,[c] %	dimensionality of network
1	Cl	DIA	2	180	3.04	16.7	1
2	Br	DIA	2	180	3.16	16.8	1
3	Cl	DIA	3	82, 90	3.09	15.3	2
	Cl	TIE	3	81	3.24/3.34	11.2/8.5	
4	Br	DIA	3	81, 89	3.19	16.1	2
	Br	TIE	3	79	3.33/3.40	12.3/10.5	
5	Br	TIE	4	83, 97	3.23	15.0	2
	$AuBr_2$	TIE	4	81, 86, 97	3.27/3.37	10.2/7.4	
6	Cl	*p*BIB	2	180	3.11	14.8	1
7	Br	TIE	2	126	3.22/3.26	15.3/14.2	2
8	Br	TIE	8	69, 74, 106, 111	3.71	2.4	3
	I	TIE	6	74, 75, 80, 88, 90, 126, 139	3.45/3.74	14.6/7.4	
$PPh_4[Cl(DIA)_2]$[d]	Cl	DIA	4	79, 112, 139	3.18/3.32	12.9/9.0	2
$PPh_4[Br(DIA)_2]$[d]	Br	DIA	4	77, 110, 136	3.24/3.39	14.7/10.8	2
$PPh_4[I(DIA)_2]$[d]	I	DIA	4	75, 106, 130	3.34/3.52	17.3/12.9	2

[a] The number of neutral molecules by which the anion is coordinated. [b] The coordination angle around the anion X. [c] Reduction ratio against the van der Waals contact. [d] Reference 8.

and shape of the neutral molecule are fixed, the architecture of the supramolecular assembly is decided by the coordination motifs. As coordination motifs, we should consider the distance, the number, and the angle around the anions. When we take it into consideration that the Cl^- and Br^- analogues often produce isomorphous structures, small deviation of the I···X distances described in the previous paragraph seem not to be very crucial for the crystal packing. On the other hand, the difference of the coordination number and angle changes the topology of the supramolecular framework drastically. In this point of view, we can conclude that the coordination number and angle around the anions are more important for the total packing than the distance. It is plausible, however, that the number and the angle do not have clear relation to each other. This is a consequence of unique nature of the halogen−halogen coordination. On the basis of these observations, it should be mentioned that the variety of the supramolecular structures described in this paper originates in the flexibility of the coordination number and angle that the anions adapt. This flexibility will provide further development of multicomponent molecular conductors with various supramolecular structures and donor arrangements.

Conclusion

We demonstrated that the novel polymeric configurations based on anions and *neutral* Lewis-acidic molecules provided conductive cation-radical salts with new types of donor arrangements. These new arrangements led to interesting band structures and transport properties. On these results, we are convinced that the supramolecular assemblies can play an important role in the survey of novel molecular conductors. In the future survey, further expansion will be made with various donor systems. In addition, the size of the neutral molecule as well as the number and geometry with which the iodine atoms are attached to the molecular skeleton will be also variable. An overview of the molecular packing resulted in some scopes for the architecture of the crystal. Examination of much more cases will allow us to design "tailor-made" anion networks to accomplish desired donor arrangements.

Among polymeric anion layers, this type of supramolecular system possesses an advantage over conventional ones such as $Cu^{2+}[N(CN)_2^-]Br^-$,[33] because there is less need to adjust the charge in designing the polymeric framework. In addition, the physical and chemical properties of the neutral molecules (for example, electronic polarization of soft iodine atoms in DIA, TIE, and *p*BIB) which can be tuned by the choice of functional groups and molecular shape should open new aspects to molecular conductors.

Acknowledgment. The authors are deeply indebted to Prof. Takehiko Mori of Tokyo Institute of Technology and Dr. Masafumi Tamura of Toho University for active discussions with us.

Supporting Information Available: Figures of the crystal structures, the resistivity data, and the density of states for the salt **5**, tables of the conditions for the crystal growth and size of the DIA/TIE unit, and X-ray structure reports of the salts (12 pages, print/PDF). See any current masthead page for ordering information and Web access instructions.

JA980024U

(33) Kini, A. M.; Geiser, U.; Wang, H. H.; Carlson, K. K.; Williams, J. M.; Kwok, W. K.; Vandervoort, K. G.; Thompson, J. E.; Stupka, D. L.; Jung, D.; Whangbo, M. H. *Inorg. Chem.* **1990**, *29*, 2555−2557.